

Single Molecules as Probes of Lipid Membrane Microenvironments

Chad E. Talley and Robert C. Dunn*

Department of Chemistry, University of Kansas, Malott Hall, Lawrence, Kansas 66045

Received: July 28, 1999; In Final Form: September 20, 1999

The single-molecule dynamics of the membrane probe diIC₁₈ dispersed in well-controlled lipid environments were studied. Lipid monolayers and bilayers of DPPC, transferred onto a solid substrate using the Langmuir–Blodgett technique, were utilized to systematically control the environment around single diIC₁₈ molecules. The single-molecule emission trajectories revealed large intensity fluctuations that were strongly coupled to the lipid environment surrounding the probe molecule. For example, as the surface pressure of a DPPC monolayer was increased from the liquid-expanded/liquid-condensed ($\pi = 5$ mN/m) region to the solid condensed ($\pi = 30$ mN/m) region, the characteristic fluorescence fluctuation times increased from approximately 440 ms to over 1 s. For bilayer films, we found characteristic fluctuation times on the order of 2 s, regardless of which side of the bilayer the probe molecule resided. The monolayer and bilayer results are most consistent with a mechanism for intensity fluctuations driven by small twisting motions in the diIC₁₈ probe molecule that modify its emission properties. Comparison of the measured time scales with results from NMR studies suggest that the observed single-molecule dynamics are associated with director fluctuations arising from collective motions of the lipid tailgroups. These results clearly reveal an environmental dependence in the single-molecule emission trajectories that can provide a new tool for studying membrane microenvironments and dynamics.

Introduction

Over the past several years single-molecule spectroscopy has emerged as a powerful technique for investigating systems free from the ensemble averaging present in bulk spectroscopic measurements.^{1,2} In the absence of averaging, triplet blinking, photon-antibunching, spectral diffusion, and a collection of other time dependent mechanisms that modify the single-molecule emission characteristics have become observable.

Early work at cryogenic temperatures revealed that both spontaneous and photoinduced processes can lead to changes in the emission characteristics of a probe molecule. The spontaneous processes are observed in both crystalline and amorphous solids at low temperature and can arise from several mechanisms. For instance, fluctuations in the molecular environment around the probe molecule can shift the single-molecule spectrum as a function of time, a process referred to as spectral diffusion.^{3,4} Low probability intersystem crossing events from the excited singlet state to the triplet manifold can also affect the single-molecule emission by leading to off periods in the fluorescence intensity.^{5,6} These and other mechanisms can lead to time dependent jumps in the total emission intensity from a single molecule.

Similar fluorescence intensity fluctuations are ubiquitous in room-temperature studies on single molecules. Both far-field and near-field techniques have been utilized to study single molecules at room temperature in various host environments.^{7–17} As in the low-temperature work, evidence for both spontaneous and photoinduced processes have been found to affect the emission characteristics. Many of these processes are sensitive to the immediate environment around the probe molecule, which has generated a great deal of interest in using single molecules as molecular level probes of their surroundings. Mechanisms such as spectral diffusion or conformational-induced changes in the emission yield are intimately tied to fluctuations in the

environment. Single-molecule emission trajectories, therefore, may provide a new tool for probing sample microenvironments once these processes have been characterized for specific probe molecules in well-defined and controllable environments.

Langmuir–Blodgett (LB) films of lipids transferred onto a substrate provide a convenient framework to study single-molecule fluctuations in environments that can be systematically altered in a highly controlled manner. The phase domain structure and lipid orientation in these films have been extensively characterized both experimentally and theoretically as a function of surface pressure and film constituents.^{18–27} Moreover, many of the dynamic processes in lipid films have been studied with techniques such as NMR.^{28–31} These films, therefore, provide well-controlled host environments in which single-molecule dynamics can be systematically studied and the results compared directly with previous findings collected with complementary techniques.

In this report, single-molecule intensity trajectories of diIC₁₈ are studied in LB films of DPPC. Both monolayers and bilayers supported on mica substrates are studied as a function of film pressure and subphase conditions. We find that the time scales of the single-molecule intensity fluctuations are strongly coupled with the film conditions, suggesting single-molecule measurements will be a powerful technique for probing membrane microenvironments. Polarization measurements and two-color measurements are used to rule out rotational diffusion and spectral diffusion, respectively, as the dominant source of the observed fluctuations. The time scales of the fluctuations and the results from the bilayer studies are also inconsistent with a triplet blinking mechanism. Instead, the results support a mechanism in which the emission fluctuations are strongly coupled with twisting motions in diIC₁₈ that alter the emission yield. Comparison with NMR data on similar membranes suggests that the observed emission jumps are associated with

slow collective lateral fluctuations of the lipid tailgroups termed director fluctuations. Thus, the single-molecule intensity trajectories probe the freedom associated with the tailgroups in the lipid film and provide a molecular level marker for film structure and dynamics.

Experimental Section

Lipid films of L- α -dipalmitoylphosphatidylcholine (DPPC) (Sigma)/ 10^{-6} mol % 1,1'-dioctadecyl-3,3,3',3'-tetramethylindocarbocyanine perchlorate (diIC₁₈) (Molecular Probes) were deposited onto freshly cleaved mica substrates using the Langmuir–Blodgett technique (Nima, model 611). DPPC/diIC₁₈ films were spread from a chloroform solution onto an aqueous subphase. The monolayer film was then compressed to the desired pressure at a rate of 100 cm²/min and transferred onto the mica substrate by vertically dipping the mica through the air–water interface at a rate of 25 mm/min. Bilayer films were prepared by subsequently depositing a second monolayer via the Langmuir–Schaeffer technique.

Samples were attached to closed-loop x – y piezo stage mounted on an inverted fluorescence microscope (Zeiss Axiovert 135TV). The 514 nm line of an argon ion laser (Liconix 5000 series) was passed through a holographic grating (Kaiser Optical) to remove unwanted plasma lines followed by a combination of a $\lambda/2$ and $\lambda/4$ waveplates to control the polarization. The intensity of the laser beam was actively stabilized (ThorLabs, CR200-A) to control long-term drift of the excitation power. The inverted microscope was configured for epi-illumination using a dichroic beam splitter (Chroma) and a high numerical aperture oil immersion objective (Zeiss Fluor 100 \times , 1.3 NA). The excitation light was adjusted to yield a power density of 500 W/cm² at the sample surface. The sample was raster scanned using the x – y piezo stage and conventional scanning electronics (Digital Instruments, Nanoscope IIIa). Sample fluorescence was separated from residual laser excitation (Chroma) and imaged onto a high quantum efficiency avalanche photodiode detector (EG&G SPCM-AQ-151). The fluorescence signal was sampled at a rate of 50 Hz using custom-designed counting electronics. All experiments were carried out at a relative humidity of 20% \pm 10%.

The two-color emission studies were carried out by splitting the collected fluorescence with a dichroic beam splitter centered near the peak of the bulk emission band (565 nm). Each emission signal was simultaneously detected using separate avalanche photodiode detectors. For the polarization modulation studies, the 514 nm line of the argon ion laser was sent through a 50/50 beam splitter. Each beam was polarized to greater than 100:1 using a combination of $\lambda/2$ and $\lambda/4$ waveplates. A mechanical chopper (Newport) was utilized to switch between the two orthogonal polarizations before the beams were recombined with a 50/50 beam splitter and coupled into a single mode optical fiber that channeled the light into the microscope.

Results

Figure 1A shows a typical pressure isotherm for DPPC at room temperature with an inset schematically showing the general order at the two points where the monolayers were transferred onto mica. These two regions of the pressure isotherm were chosen for comparison and correspond to the liquid-expanded/liquid-condensed (LE/LC, $\pi = 5$ mN/m) coexistence region and the solid-condensed (SC, $\pi = 30$ mN/m) region of the pressure isotherm. The molecular structures of the lipid and probe molecules are shown in Figure 1B.

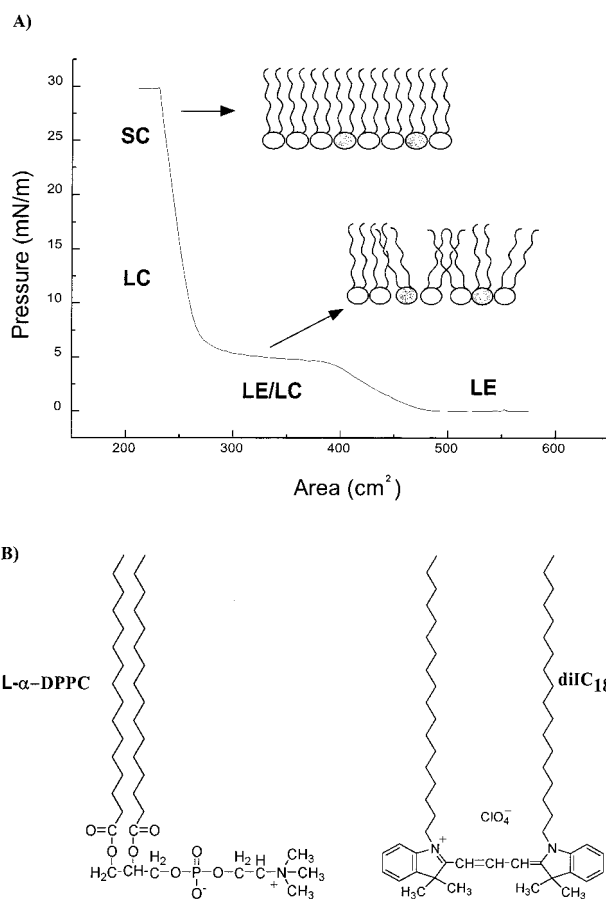


Figure 1. (A) Typical pressure isotherm of DPPC at room temperature. The phases along the isotherm are identified as liquid expanded (LE), liquid condensed (LC), and solid condensed (SC). The arrows mark the regions in the isotherm where films were transferred onto mica for study. (B) The molecular structures for DPPC and the fluorescent membrane probe, diIC₁₈.

The lipid–dye ratio was adjusted to DPPC/ 10^{-6} mol % diIC₁₈, which gives a coverage of approximately 0.5 diIC₁₈ molecules/ μm^2 . At these low concentrations, the dye does not affect the shape of the pressure isotherm or the phase partitioning in the lipid film. Both far-field and near-field fluorescence studies have shown that the fluorescent diIC₁₈ selectively partitions into the less ordered LE phase at the lower pressures. Thus, even though films prepared in the LE/LC coexistence region are heterogeneous, the probe dye molecules are confined to the LE regions of the film. At higher film pressures, the dye is forced into the SC phase. Therefore, the studies discussed below will be comparing the intensity trajectories for dye molecules surrounded by the LE lipid phase and those in a more rigid and ordered SC lipid phase. This represents a large change in molecular area, going from approximately 65 Å² in the LE phase to 45 Å² in the SC phase.^{32–35} Under each experimental condition, several hundred molecules were studied. The number of molecules that lived long enough to give good counting statistics are listed in Table 1.

Figure 2 schematically shows the four different lipid environments characterized in this study. For the bilayer studies, the probe diIC₁₈ molecules were selectively doped into one side of the bilayer. The side of the bilayer containing the dye was transferred at $\pi = 5$ mN/m, while the adjacent side was transferred at $\pi = 30$ mN/m. We have previously shown that the phase domain structure is preserved in bilayers formed with the Langmuir–Schaeffer technique.²⁶ These films, therefore,

TABLE 1: Tabulation of the Results from the Single-Molecule Experiments^a

film condition	subphase	τ_1 (s)	τ_2 (s)	N
liquid expanded phase	10 mM MgCl ₂	0.44 ± 0.10	14.2 ± 3.9	66
solid condensed phase	10 mM MgCl ₂	1.17 ± 0.27	24.1 ± 5.5	48
liquid expanded phase	water	0.77 ± 0.22	18.2 ± 6.3	46
solid condensed phase	water	1.31 ± 0.36	13.1 ± 4.1	37
bilayer (probe on bottom)	water	2.06 ± 0.50	41.9 ± 12.5	43
bilayer (probe on top)	water	2.14 ± 0.64	28.9 ± 11.2	32

^a Listed are the phase of the lipid film, subphase conditions, the time constants resulting from the biexponential fits of the intensity autocorrelations (τ_1 and τ_2), and the number of molecules N that survived long enough to analyze. Errors correspond to the 90% confidence intervals.

provide samples in which the phase environment around the probe molecule remains LE while the tailgroups are restricted due to the interactions between the bilayer leaflets.

Finally, two different subphases were investigated in the monolayer studies. DPPC monolayers were prepared using both a pure water subphase and a subphase containing 10 mM MgCl₂. It has been previously shown that the presence of divalent cations in the subphase can modify the interactions between DPPC and the mica surface.^{27,36–39} Comparing monolayers transferred from different subphases therefore provides further insight into the environmental contributions to the intensity fluctuations. Table 1 lists all the film conditions investigated in this study.

Parts A and C of Figure 3 show representative fluorescence intensity traces for a diIC₁₈ molecule in the indicated lipid environment. The fluorescence intensity trajectories show fluctuations that are indicative of single-molecule dynamics. To extract the important time scales from the single-molecule trajectories and quantitatively compare the results between different lipid film conditions, the intensity traces were analyzed using the well-known normalized intensity autocorrelation function.

$$C(t) = \frac{\sum_{i=0}^N (I_i - \bar{I})(I_{i+t} - \bar{I})}{\sum_{i=0}^N (I_i - \bar{I})^2} \quad (1)$$

In eq 1, \bar{I} is the average intensity, I_i is the intensity at time t , and I_{i+t} is the intensity at time $t + \tau$.

As an example of the analysis, autocorrelations of the data are plotted in Figure 3B,D alongside their respective intensity trajectories. In general, the resulting autocorrelations are best fit to a biexponential decay. The average time constants resulting from biexponential fits to the individual autocorrelation functions are shown in Table 1 along with the 90% confidence intervals. Also tabulated are the film condition, subphase, and number of molecules analyzed.

Both rotational and spectral diffusion of the molecule in the film can lead to intensity fluctuations similar to those shown in Figure 3. To check for rotational diffusion, the excitation polarization was modulated between parallel and perpendicular polarization at 1 Hz while the fluorescence from a single molecule was collected. The results from a typical experiment are shown in Figure 4 for a probe molecule in a DPPC monolayer deposited at $\pi = 5$ mN/m. The observed emission is highest for the parallel polarization where there is maximal

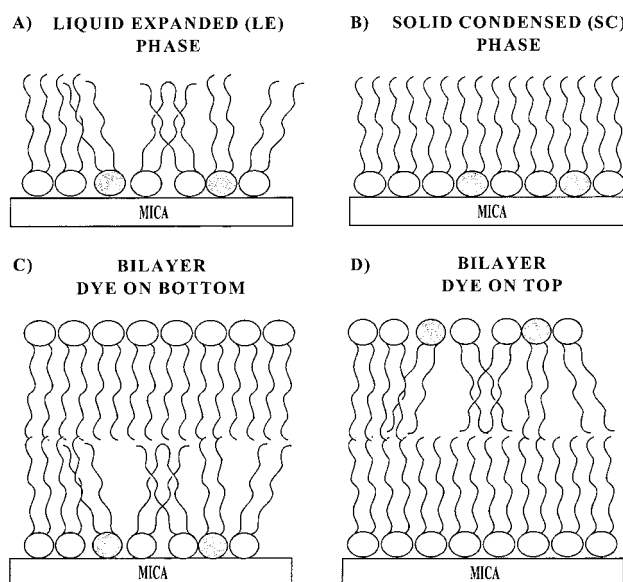


Figure 2. Schematic representations of the various film conditions utilized to study the environmental dependence in the single-molecule intensity fluctuations. The diIC₁₈ probe molecule (darkened headgroup) was doped into the DPPC films at a concentration of 10^{-6} mol %.

overlap between the excitation polarization and the transition dipole moment of the particular molecule. The signal drops to the background level when the polarization is rotated 90°. As seen in Figure 4, the time dependent intensity fluctuations are present during parallel excitation while the signal from perpendicular excitation remains near the background level. This lack of correlation suggests that the observed intensity fluctuations are not the result of rotational diffusion of diIC₁₈ in the membrane plane.

To investigate the contribution from spectral diffusion, the blue and red regions of the emission spectrum were separated and detected simultaneously. This method offers higher time resolution than collecting the entire spectrum as a function of time and has been shown previously to be sensitive to spectral diffusion.⁴⁰ Figure 5 shows the results from a typical experiment on diIC₁₈ in a DPPC monolayer transferred at $\pi = 5$ mN/m. The normalized intensity traces exhibit large intensity fluctuations that track one another. This suggests that the spectrum is stable in time and spectral diffusion is not a major contributor to the observed intensity fluctuations.

Discussion

The results summarized in Table 1 clearly show trends in the power-independent fast time component (τ_1) of the single-molecule intensity fluctuations that are tied to the order in the lipid films. The long time component (τ_2), which is power dependent, has been shown by others to arise from photoinduced processes and will not be discussed further here.¹⁵ In general, as the order in the lipid film increases, we observe an increase in the τ_1 times. For example, diIC₁₈ molecules dispersed in DPPC monolayers transferred from a water subphase have a τ_1 time that increases from 770 ms in the LE phase to 1.31 s in the SC phase. Similarly, when monolayers are transferred from a subphase containing 10 mM MgCl₂, the τ_1 times increase from 440 ms in the LE phase to 1.17 s in the SC phase. Moreover, we observe a dramatic increase in the τ_1 times when diIC₁₈ is doped into bilayer films, even though the probe molecule remains in the LE phase. The τ_1 times increase to approximately 2 s, regardless of which side of the membrane the probe molecules reside.

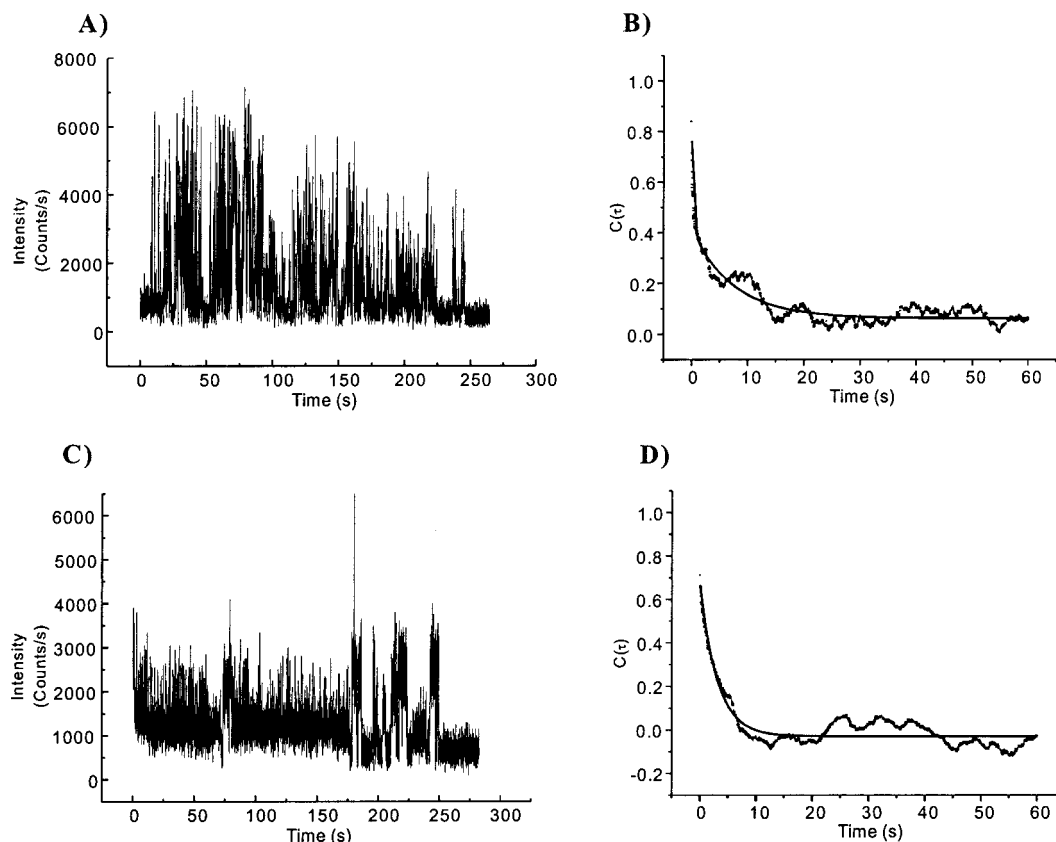


Figure 3. (A) Representative single-molecule intensity trace for diIC₁₈ in the LE phase of a DPPC monolayer. (B) Autocorrelation of the intensity trace shown in (A). The intensity autocorrelation is fit to a biexponential function (solid line) with time constants of $\tau_1 = 290$ ms and $\tau_2 = 7.60$ s. (C) and (D) show similar results for a probe molecule in the bottom leaflet of a bilayer membrane. The intensity autocorrelation shown in (D) is fit with decay times of $\tau_1 = 3.10$ s and $\tau_2 = 11.0$ s.

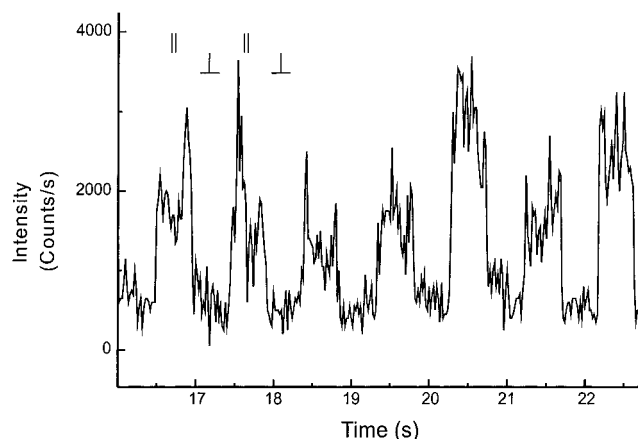


Figure 4. To check for rotational diffusion, the excitation polarization was modulated between parallel and perpendicular polarizations while the total emission intensity was collected from a single molecule. As seen in the intensity trace, large fluctuations are observed for parallel-polarized excitation while the intensity remains near the background for perpendicular-polarized excitation.

As will be discussed later, we believe that all of these results can be understood within a mechanism in which the fast intensity fluctuations are driven by small twisting motions of the diIC₁₈ probe molecule that modifies its emission yield. This mechanism should be intimately coupled with the tailgroup freedom of the surrounding lipid matrix and has recently been invoked by Weston and Buratto to explain the observed fluctuations of diIC₁₂ absorbed on a glass substrate.¹³ Before discussing this mechanism and its potential for observing lipid

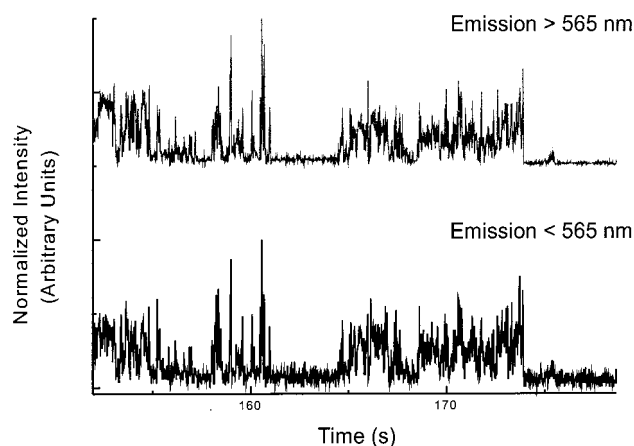


Figure 5. To test for spectral diffusion, the emission was split with a dichroic beam splitter centered at 565 nm and detected simultaneously with two detectors. The correlation between the intensity fluctuations on the blue and red sides of the emission spectrum suggests that the intensity fluctuations are not dominated by spectral diffusion.

membrane dynamics, however, we will first consider other mechanisms that may be contributing to the observed dynamics.

Several environmentally dependent processes can lead to the observed fluctuations, and it is possible that more than one photophysical process is contributing to the dynamics characterized in this study. In the next sections we consider the possible contributions from mechanisms previously established in other single-molecule studies that lead to similar intensity fluctuations. These mechanisms include rotational diffusion, spectral diffusion, and triplet blinking, all of which can conceivably yield

the environmental dependencies observed in this study.

Rotational Diffusion. Rotational diffusion of diIC₁₈ in the lipid film can lead to intensity fluctuations by changing the overlap between the polarized excitation light and the transition dipole moment of the probe molecule. Rotational diffusion would also be expected to yield the same trends observed in the data, namely an increase in τ_1 times as the film density increases. As others have shown, this can be probed by modulating the excitation light between parallel and perpendicular polarizations.^{12,40} Any rotation of the molecule will lead to a decrease in emission from one polarization with a concomitant increase in the other. Figure 4 shows the results from a typical experiment in which the excitation polarization is modulated while the total emission is collected. As seen in Figure 4, large fluctuations in the emission intensity are seen for the parallel excitation while there are no related changes in the emission from the perpendicular excitation. This shows that the intensity fluctuations are still present but are not arising from rotational freedom of the probe molecule in the lipid film. It should also be mentioned that lateral diffusion of the probe molecules was not observed in any of the film conditions studied. This was checked through repeated imaging of the same area with confocal microscopy and with higher resolution studies using near-field scanning optical microscopy.

Spectral Diffusion. The time scales of the intensity fluctuations observed in this study (hundreds of milliseconds) are consistent with those previously reported for the spectral diffusion of sulforhodamine 101 in a polymer host.¹⁵ For single wavelength studies this spectral wandering changes the molecular absorption cross-section at the fixed excitation frequency which, in turn, changes the emission intensity as a function of time. Spectral diffusion can be probed through measurements of the spectra as a function of time¹⁵ or, on a faster time scale, through two-channel experiments in which the blue and red regions of the spectra are detected simultaneously.⁴⁰

Figure 5 shows the results of a two-channel experiment for diIC₁₈ in the LE lipid phase. As can be seen, the simultaneous recordings reveal large intensity jumps that are correlated in the two spectral regions. Spectral diffusion would lead to an anticorrelation in the two-channel experiment that is not supported by the data shown in Figure 5. These results suggest that spectral diffusion is not the dominant source of the diIC₁₈ intensity fluctuations observed in this study.

Triplet Blinking. Triplet blinking arises from low probability transitions to the long-lived triplet manifold, which leads to dark periods in the intensity trajectory. Evidence for triplet blinking has been found in several single-molecule studies and recently Barbara and co-workers have found this to be the dominant source of intensity fluctuations for diIC₁₂ in films of PMMA.⁷ Several lines of evidence, however, suggest that in our specific experimental arrangement this is not the dominant mechanism leading to the intensity fluctuations.

Under the triplet blinking mechanism, autocorrelations of the intensity trajectories typically show decay times ranging from hundreds of microseconds to milliseconds, mapping the triplet lifetime. For example, several single-molecule studies have found millisecond lifetimes for the triplet state of diIC₁₂ molecules dispersed in PMMA.^{7,13,41} These times are similar to bulk measurements on related dyes that found triplet lifetimes on the tens of millisecond time scale.⁴² For all lipid film conditions studied, however, we find τ_1 times that are significantly longer than times characteristic for triplet blinking (see Table 1). At the extreme are the bilayer results in which the τ_1

times increase to the order of seconds, clearly much longer than that expected for triplet blinking.

In addition, we also find no statistical difference between the τ_1 times for molecules located in the bottom monolayer of the bilayer and those residing in the upper monolayer exposed to air. As many studies have shown, intensity fluctuations arising from triplet blinking are very sensitive to the accessibility of oxygen. Molecular oxygen is a well-known quencher of the triplet state and therefore influences the lifetime of the dark state. One would expect, therefore, that probe molecules located on the exposed side of the bilayer, which are more accessible to oxygen, should exhibit shorter fluctuation times than those located on the bottom side of the bilayer. This is supported by electrochemical measurements on monolayers of octanol at the air/water interface showing that diffusion of oxygen across the monolayer is slowed by a factor of 2 as the surface pressure is increased from 5 to 50 mN/m.⁴³ The insensitivity of the correlation times to the probe molecule location in the bilayer, therefore, suggests a mechanism other than triplet blinking is dominating the dynamics.

At first, these results would seem at odds with recent results on the related dye molecule diIC₁₂, which suggested that the dynamics are dominated by triplet blinking.⁷ These measurements revealed fluctuation times on the order of several milliseconds, which agrees with previously measured triplet blinking times.^{9,41} The differences between our results and the previously reported intensity fluctuations may be attributable to variations in the excitation rate, since the contribution from triplet blinking becomes greater as the excitation rate nears saturation.¹ In fact, when we double our excitation power to 1000 W/cm² and increase the sample rate to 1 kHz we find evidence for an additional decay time on the order of milliseconds in a small fraction of the molecules. This new component is consistent with that previously assigned to triplet blinking. As the excitation power is reduced to that used in this study (500 W/cm²) while the fast sampling rate (1 kHz) is maintained, however, this component is rarely observed and the fluctuations are dominated by the longer time components listed in Table 1. Taken together, these results suggest that triplet blinking is not dominating the observed dynamics in this particular study.

Conformational Changes. Our data are most consistent with a mechanism for intensity fluctuations recently proposed by Weston and Buratto for diIC₁₂ absorbed on glass.¹³ The results from these experiments suggested that a twisting motion around the carbon chain linking the indole rings leads to changes in the emission yield, producing fluctuations on the millisecond time scale. For our experimental arrangement, these conformational changes should be sensitive to the freedom in the tailgroups of diIC₁₈ and those of the surrounding DPPC. Low-angle X-ray and neutron scattering data indicate that the molecular area of DPPC decreases from approximately 65 Å² in the LE phase to 45 Å² in the SC phase.^{32–35} The dramatic increase in the τ_1 times as the film is compressed, therefore, is consistent with a decrease in the tailgroup freedom of the probe molecule, thus reducing the emission fluctuations arising from twisting motions of the chromophore.

The twisting mechanism is also supported by the trends seen in the bilayer results. In forming the bilayers, the side containing the probe molecule was kept in the LE phase while the side opposite was deposited in the SC phase. Despite the probe molecule being surrounded by LE phase lipid, we find that the τ_1 times increase to approximately 2 s regardless of the side of the bilayer on which the probe molecule is located. This is

consistent with the advent of interactions between the tailgroups from the two sides of the bilayer, which restricts the tailgroup motions and, therefore, the twisting motion in the diIC₁₈. Moreover, the lack of sensitivity in the τ_1 times to location in the bilayer suggests that the fluctuations are less sensitive to the presence of the substrate and more sensitive to the lipid tailgroup interactions.

It is also interesting to compare the results obtained for DPPC monolayers prepared from different subphases. Comparing monolayers prepared at the same surface pressure ($\pi = 5$ mN/m) indicates that the τ_1 times decrease from 770 ms when transferred from a pure water subphase to 440 ms upon transfer from a subphase of 10 mM MgCl₂. Since these monolayers are transferred at the same pressure, the lipid density remains comparable, but the data shown in Table 1 indicate almost a 2-fold difference in the τ_1 times. A similar trend is seen at the higher surface pressure although the difference is much less significant.

These differences are consistent with several studies that have demonstrated the influence of subphase cations on the lipid–substrate interactions.^{27,36–39} Divalent cations are known to bind to the headgroup of the zwitterionic DPPC and replace the potassium ions at the surface of the mica substrate. As the DPPC headgroups approach the mica substrate, the respective divalent cations and their associated hydration spheres come into close contact. The short-range repulsive hydration forces between these two surfaces tend to destabilize the film and weaken the interactions between the DPPC and mica surface. The decrease in the τ_1 times observed for monolayers transferred from MgCl₂, therefore, is consistent with an increase in the fluidity in the lipid film arising from these decreased lipid–substrate interactions. At higher surface pressures, the density of the film offsets this mechanism and the τ_1 times converge to approximately the same value for both subphase conditions.

It is interesting to compare the time scales measured here with previous dynamic studies on lipid films. The relevant time scales in lipid films span many orders of magnitude ranging from very fast processes such as trans–gauche isomerization and bond vibrations that occur on the subnanosecond time scale to extremely slow events such as lipid flip-flop across a bilayer, which can take from minutes to days. Both the fast and slow motions of lipid films have been studied extensively using NMR techniques.^{28–31} Usually, for motions with correlation times less than 10^{-8} s the longitudinal relaxation time (T_1) is utilized. Motions long on the NMR time scale are probed through analysis of the transverse relaxation time (T_2), although the T_1 time can also yield information on the low-frequency motions. The slow lipid film processes measured with NMR involve motions such as lateral diffusion, membrane undulations, and director fluctuations, all of which can yield signals in the kilohertz regime.

The slow hundreds of milliseconds fluctuations captured in the single-molecule experiments are most consistent with the director fluctuations implicated in several NMR studies. These motions involve many lipids and are thought to arise from collective lateral fluctuations of the lipid tailgroups. These are the type of motions that would be expected to strongly affect the emission properties of the diIC₁₈ probe molecule through the twisting mechanism discussed earlier. Generally, NMR studies find that these motions have correlation times longer than 10^{-4} s, which is also consistent with the single-molecule correlation times reported here.^{29,30}

Given the interest in the role of lipids in modulating the activity of membrane-bound enzymes, receptors, or transporters,

the characterization of these low-frequency collective motions is of considerable importance. It has been suggested that the activity of membrane proteins can be coupled with these slow cooperative motions and that long-range protein–protein interactions may be communicated through collective lipid dynamics.²⁹ With the advent of single-molecule spectroscopy, characterizing these motions as a function of membrane constituents opens new avenues for exploring their influence.

There is also a great deal of interest in understanding the role of membrane constituents such as cholesterol in modifying the structure of lipid membranes. Single-molecule measurements similar to those reported here should provide a new microscopic view into the role of cholesterol in modifying the dynamics of lipid membranes. Moreover, it may be possible to tune the dye molecule such that new and complementary dynamic processes can be revealed. For instance, choosing a probe molecule known to spectrally diffuse may provide a probe of more local fluctuations in these membranes, which can complement the results reported here. These studies are currently underway.

Conclusions

Single-molecule fluorescence intensity fluctuations of diIC₁₈ dispersed in DPPC monolayers and bilayers have been studied as a function of film surface pressure and subphase constituents. By systematically changing the surface pressure in these lipid films, the influence of the environment on the single-molecule fluorescence trajectories has been studied. We have shown that the fluctuations are dependent on the specific lipid environment with correlation times increasing as the order in the film increases. The results from two-color and polarization measurements suggest that spectral diffusion and rotational diffusion, respectively, are not contributing significantly to the observed dynamics. Instead, our results are most consistent with a model in which the intensity fluctuations are driven by small twisting motions around the carbon chain linking the two indole rings of the diIC₁₈ molecule, causing fluctuations in the emission yield. These motions are particularly sensitive to the degrees of freedom accessible to the lipid tailgroups and are consistent with the increased correlation times observed in both the monolayer and bilayer membranes. Comparison with NMR studies suggests that the single-molecule trajectories are probing a collective motion in the lipid hydrocarbon chains. The extension of these results to more complex multicomponent membranes containing proteins, cholesterol, or other lipids is straightforward and should provide new insights into the low-frequency dynamics of these systems.

Acknowledgment. We thank Dr. David Ehrlich for help in developing the analysis software and the University of Kansas Instrument Design Laboratory for designing the counting electronics. We gratefully acknowledge the support of the NSF (CHE-9612730).

Note Added in Proof: Since the submission of this manuscript, we have characterized the orientation of single TRITC-DHPE probe molecules in DPPC films using near-field scanning optical microscopy. At DPPC film pressures similar to those discussed here, we find no significant change in the probe orientation within the film. This may suggest that the probe remains trapped in LE domains that persist even at high surface pressures. The results presented here may therefore reflect a decrease in probe freedom associated with these smaller LE domains at high surface pressures. We are currently carrying

out studies at pressures near film collapse which may provide further insight into the particular environment around the probe molecule.

References and Notes

- (1) Xie, X. S.; Trautman, J. K. *Annu. Rev. Phys. Chem.* **1998**, *49*, 441–480.
- (2) Plakhotnik, T.; Donley, E. A.; Wild, U. P. *Annu. Rev. Phys. Chem.* **1997**, *48*, 181–212.
- (3) Ambrose, W. P.; Moerner, W. E. *Nature* **1991**, *349*, 225–227.
- (4) Ambrose, W. P.; Basche, T.; Moerner, W. E. *J. Chem. Phys.* **1991**, *95*, 7150–7163.
- (5) Basché, T.; Kummer, S.; Brauchle, C. *Nature* **1995**, *373*, 132–134.
- (6) Bernard, J.; Fleury, L.; Talon, H.; Orrit, M. *J. Chem. Phys.* **1993**, *98*, 850–859.
- (7) Yip, W.-T.; Hu, D.; Yu, J.; Vanden Bout, D. A.; Barbara, P. F. *J. Phys. Chem.* **1998**, *102*, 7564–7575.
- (8) Ruiter, A. G. T.; Veerman, J. A.; Garcia-Parajo, M. F.; van Hulst, N. F. *J. Phys. Chem. A* **1997**, *101*, 7318–7323.
- (9) Ha, T.; Enderle, T.; Chemla, D. S.; Selvin, P. R.; Weiss, S. *Chem. Phys. Lett.* **1997**, *271*, 1–5.
- (10) Wang, H.; Bardo, A. M.; Collinson, M. M.; Higgins, D. A. *J. Phys. Chem. B* **1998**, *102*, 7231–7237.
- (11) Schmidt, T.; Schütz, G. J.; Baumgartner, W.; Gruber, H. J.; Schindler, H. *J. Phys. Chem.* **1995**, *99*, 17662–17668.
- (12) Xie, X. S.; Dunn, R. C. *Science* **1994**, *265*, 361–364.
- (13) Weston, K. D.; Buratto, S. K. *J. Phys. Chem. A* **1998**, *102*, 3635–3638.
- (14) Macklin, J. J.; Trautman, J. K.; Harris, T. D.; Brus, L. E. *Science* **1996**, *272*, 255–259.
- (15) Lu, H. P.; Xie, X. S. *Nature* **1997**, *385*, 143–146.
- (16) Trautman, J. K.; Macklin, J. J. *Chem. Phys.* **1996**, *205*, 221–229.
- (17) Trautman, J. K.; Macklin, J. J.; Brus, L. E.; Betzig, E. *Nature* **1994**, *369*, 40–42.
- (18) McConnell, H. M.; Tamm, L. K.; Weis, R. M. *Proc. Natl. Acad. Sci. U.S.A.* **1984**, *81*, 3249–3253.
- (19) McConnell, H. M. *Annu. Rev. Phys. Chem.* **1991**, *42*, 171–195.
- (20) Weis, R. M.; McConnell, H. M. *J. Phys. Chem.* **1985**, *89*, 4453–4459.
- (21) Lösche, M.; Sackmann, E.; Möhwald, H. *Ber. Bunsen-Ges. Phys. Chem.* **1983**, *87*, 848–852.
- (22) Tu, K.; Tobias, D. J.; Klein, M. L. *Biophys. J.* **1995**, *69*, 2558–2562.
- (23) Tu, K.; Tobias, D. J.; Blasie, J. K.; Klein, M. L. *Biophys. J.* **1996**, *70*, 595–608.
- (24) Tu, K.; Klein, M. L.; Tobias, D. J. *Biophys. J.* **1998**, *75*, 2147–2156.
- (25) Hwang, J.; Tamm, L. K.; Bohm, C.; Ramalingam, T.; Betzig, E.; Edidin, M. *Science* **1995**, *270*, 610–614.
- (26) Hollars, C. W.; Dunn, R. C. *Biophys. J.* **1998**, *75*, 342–353.
- (27) Shiku, H.; Dunn, R. C. *J. Phys. Chem. B* **1998**, *102*, 3791–3797.
- (28) Dolainsky, C.; Möps, A.; Bayerl, T. M. *J. Chem. Phys.* **1993**, *98*, 1712–1720.
- (29) Watnick, P. I.; Dea, P.; Chan, S. I. *Proc. Natl. Acad. Sci. U.S.A.* **1990**, *87*, 2082–2086.
- (30) Stohrer, J.; Gröbner, G.; Reimer, D.; Weisz, K.; Mayer, C.; Kothe, G. *J. Chem. Phys.* **1991**, *95*, 672–678.
- (31) Brown, M. F.; Seelig, J. *J. Chem. Phys.* **1979**, *70*, 5045–5053.
- (32) Koenig, B. W.; Krueger, S.; Orts, W. J.; Majkrzak, C. F.; Berk, N. F.; Silverton, J. V.; Gawrisch, K. *Langmuir* **1996**, *12*, 1343–1350.
- (33) Fischer, A.; Sackmann, E. *J. Phys.* **1984**, *45*, 517–527.
- (34) Wiener, M. C.; Suter, R. M.; Nagle, J. F. *Biophys. J.* **1989**, *55*, 315–325.
- (35) Vaknin, D.; Kjaer, K.; Als-Nielsen, J.; Lösche, M. *Biophys. J.* **1991**, *59*, 1325–1332.
- (36) Israelachvili, J. *Intermolecular and Surface Forces*, 2nd ed.; Academic Press Inc.: San Diego, 1992.
- (37) Marra, J.; Israelachvili, J. *Biochemistry* **1985**, *24*, 4608–4618.
- (38) Lis, L. J.; Parsegian, V. A.; Rand, R. P. *Biochemistry* **1981**, *20*, 1761–1770.
- (39) Pashley, R. M.; Israelachvili, J. N. *J. Colloid Interface Sci.* **1984**, *97*, 446–455.
- (40) Ha, T.; Enderle, T.; Chemla, D. S.; Selvin, P. R.; Weiss, S. *Phys. Rev. Lett.* **1996**, *77*, 3979–3982.
- (41) Trautman, J. K. Proc. Robert A. Welch Foundation, 39th Conference on Chemical Research: Nanophase Chemistry, Houston, 1996.
- (42) Buettner, A. V. *J. Chem. Phys.* **1967**, *46*, 1398–1401.
- (43) Slevin, C. J.; Ryley, S.; Walton, D. J.; Unwin, P. R. *Langmuir* **1998**, *14*, 5531–5534.